

# Reaction Mechanism Testing with Spatial and Thermal Resolutions of Methane-Air Flames

Akram Mohammad

*Department of Aerospace Engineering, King Abdulaziz University, Jeddah, Kingdom of Saudi Arabia*

*Email: amohammad4@kau.edu.sa, akrammania@gmail.com*

*Corresponding Author: akrammania@gmail.com*

**Submitted** : 05-08-2021

**Revised** : 13-01-2022

**Accepted** : 23-01-2022

## ABSTRACT

The spatial and thermal dispersals of hydroxyl (OH), formaldehyde (CH<sub>2</sub>O), and other minor species were acquired using various detailed reaction mechanisms in a weak flame of stoichiometric methane and air mixture at ambient pressure. A weak flame was simulated inside a microflow combustor with a prescribed temperature profile that released a very small amount of heat. A wide reaction zone (~ 1 cm) was observed for the methane and air flames compared to the normal/conventional flames. A detailed oxidation analysis was performed based on the normal and weak flame simulations. The computational flame structure was assessed using the experimental results available in the existing literature. Numerical modeling under experimental conditions with various detailed mechanisms predicted a similarly wide reaction zone. However, species production and consumption temperatures varied according to the different mechanisms used in the present study. The GRI mech 3.0 shows a typical two-peak heat release rate profile. The initial breakdown of the fuel is vital for such scattering. The production of OH radicals governs the initial breakdown of fuel at intermediate temperatures. The present investigation is useful for understanding the chemistry of intermediate species in different fuel-air mixtures, especially at intermediate temperatures of 800–1200 K.

**Keywords:** Mechanism testing; Weak flame; Premixed laminar flame; Species temperature dependence; Microflow combustor; etc.

## INTRODUCTION

A precise illustration of various existing and alternate fuel combustion chemistries is vital gauge the influence of fuel combustion characteristics on the performance of existing practical devices and to develop new-generation propulsion systems. Chemical kinetic research groups, such as LLNL and Aramco, have put tremendous effort into high-level comprehensive reaction mechanisms that accurately reveal the behaviors of complex reactive processes [1–6]. Methane is the lightest alkane studied for a wide range of applications [7–9]. Although the present computational fluid dynamics (CFD) packages used to model reacting flow combustion systems have seen substantial growth in recent years, most of them do not allow the incorporation of comprehensive reaction mechanisms, especially for turbulence modeling. An alternative is to reduce the existing comprehensive mechanisms (to a small chemical model) that can reproduce the combustion physics similar to that of the detailed mechanisms with reasonable accuracy. Many conventional chemical reduction models based on the elimination of unimportant species and/or reactions are available in the literature [10, 11]. This leads to the formation of reduced mechanisms suitable only for predetermined pressure and temperature conditions. To analyze both the ignition and combustion characteristics, one needs to study a range

of initial pressures and temperatures. A novel method for studying the ignition and deflagration branches using an extremely simple setup was proposed by Maruta et al. [12–18]. This simple technique competes with expensive and complex systems such as rapid compression machines (RCM) and shock tube systems. The basic combustion strategy for a microflow combustor with a prescribed wall temperature profile [12–18] is shown in Fig. 1. A 2-mm diameter quartz tube was externally heated, and a temperature gradient is formed, which helps in the stabilization of cool, weak, and normal flames at different temperatures (see Fig. 2) depending upon the fuel-oxidizer system [14, 16]. They also reported a study on RON dependencies using this simple method [12]. This system would be useful for the analysis of important species in the ignition and deflagration branches of various fuel and air mixtures.

The initial breakdown of the fuel was significantly influenced by the initial temperature of the fuel-air mixture. At low and intermediate temperatures, radicals are essential for accelerating the further breakdown of the fuel. This requires an understanding of the relationship between species distribution and temperature. This paper presents the computational results of CH<sub>2</sub>O, OH, and CH distributions over intermediate temperatures. Model predictions from various detailed mechanisms were compared with the experimental data of Shimizu et al. (2017) [16] and discussed in terms of fuel consumption to reveal the importance of OH production at intermediate temperatures.

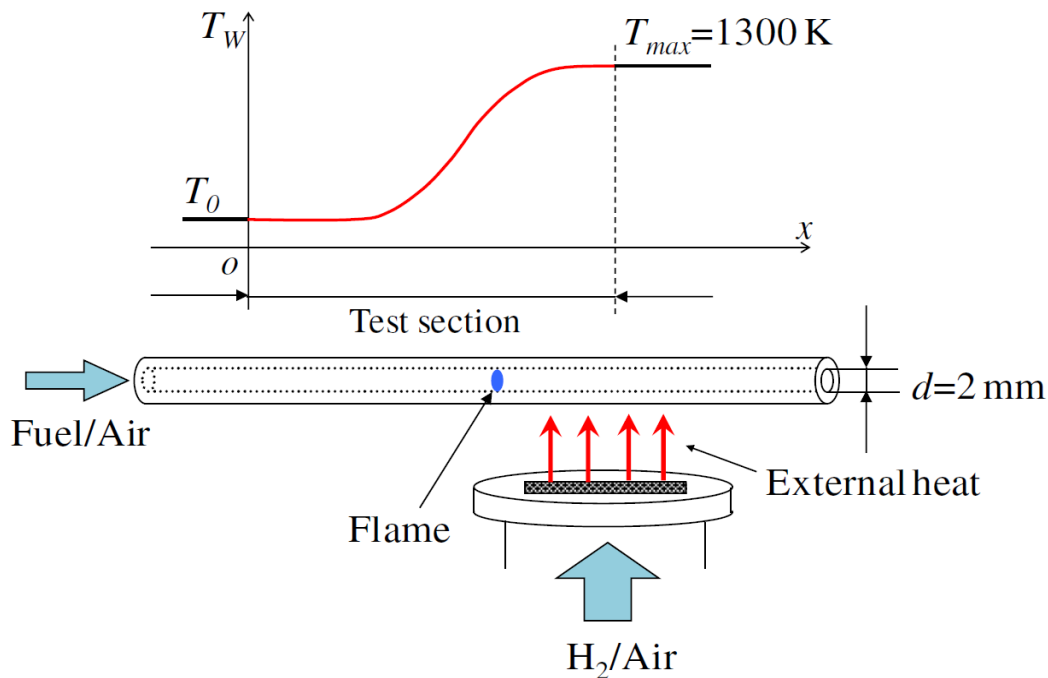


Figure 1 Microflow combustor with a prescribed temperature profile [18]

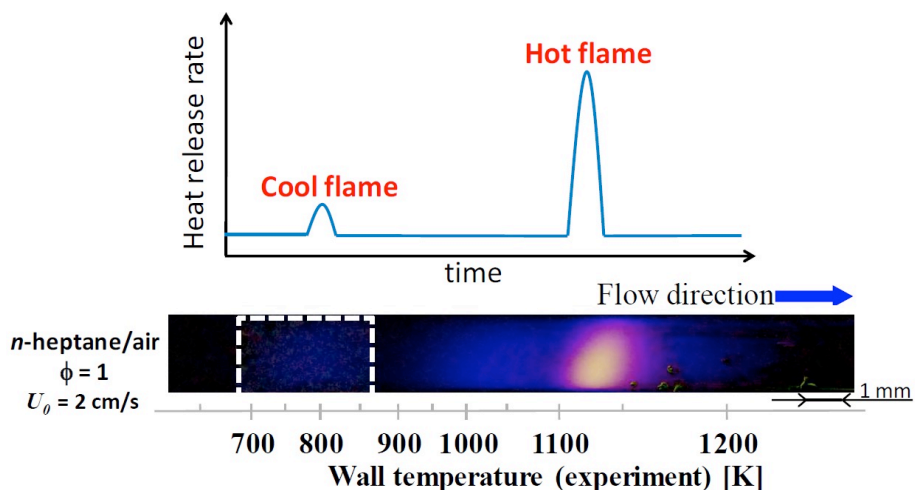


Figure 2 Separated weak flames with multi-stage ignition [18]

## Computational method

A standard PREMIX [19, 20] code was utilized to simulate the experimental conditions of the microflow combustor. This one-dimensional steady-state code was modified by introducing a thermally thick wall (temperature profile, as shown in Fig. 3, similar to the experiments) with a heat transfer source term for the energy exchange between the gas and the wall. The details of the source terms are provided in [16]. A 10-cm long computational domain was considered. The inside surface temperature of the bottom wall was measured in the axial direction. The axial coordinate also represents thermal coordinate with reference to the wall temperature profile as shown in Fig. 3.

A laminar premixed stoichiometric methane-air mixture was studied at two different velocities,  $U_{in} = 2$  cm/s and 60 cm/s, to simulate weak and normal flames, respectively. Various detailed reaction mechanisms, such as the San Diego mech [21], USC mech II [22], and GRI mech 3.0 [23], were tested under these conditions.

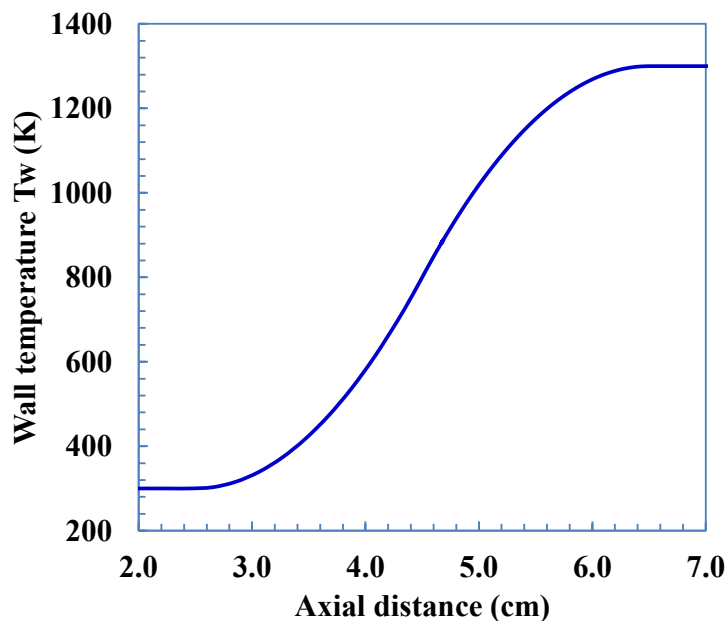


Figure 3 Wall temperature profile from computational simulation.

## Results and Discussion

## Weak flame

A weak (unconventionally wide) flame was observed at an extremely low mixture inlet velocity inside the microflow combustor. Recently, Shimizu et al. [16] and Onda et al. [24] captured weak flames by optical measurements of various species, such as OH and CH<sub>2</sub>O. Preloading of CH<sub>2</sub>O and OH was observed, as shown in Fig. 4. The mole fraction distributions of these species obtained from the present simulation showed excellent qualitative agreement with the experimental results.

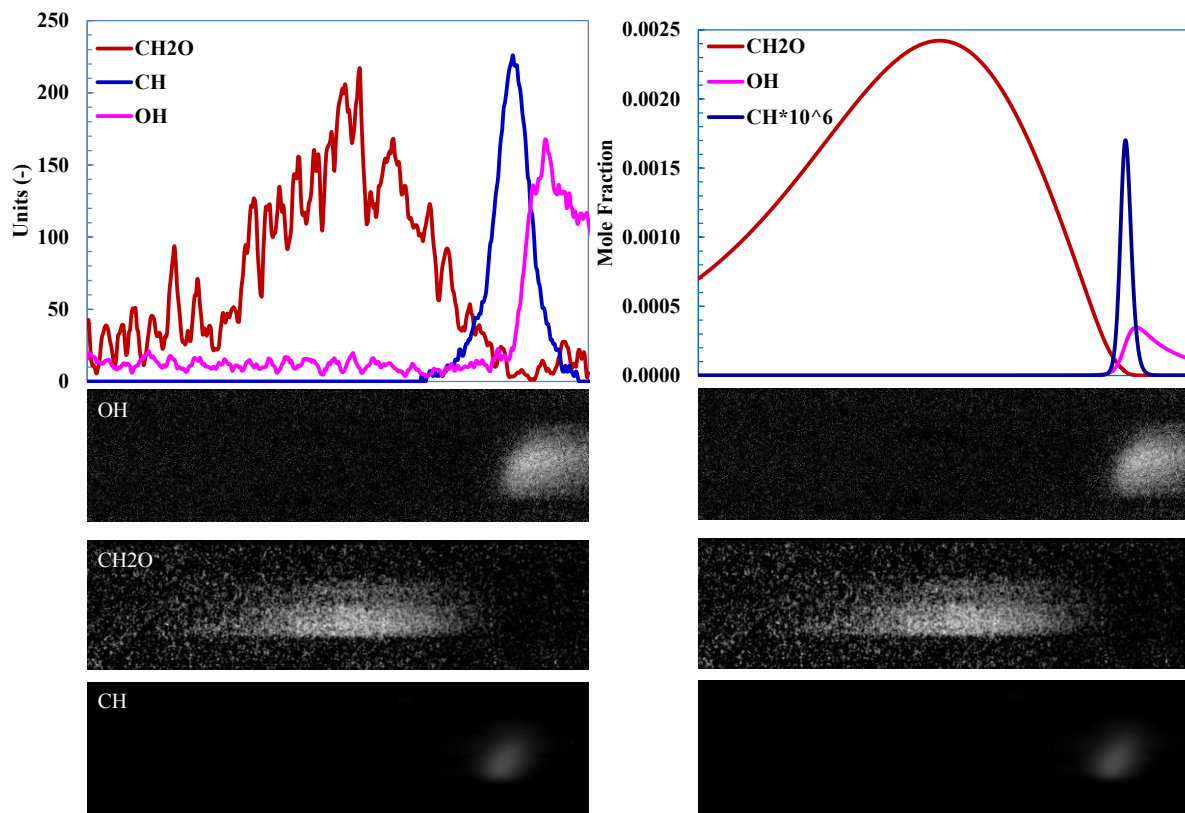


Figure 4 Chemiluminescence intensity profiles and mole fractions of CH<sub>2</sub>O, OH, and CH (using the San Diego mech) for stoichiometric methane and air weak flame at  $U_{in} = 2$  cm/s. Experimental data are taken from Shimizu et al. (2017) [16].

## Comparison of weak and normal flame

Figure 5 shows the variations in the major species for weak and normal flames. The axial coordinates

resemble thermal coordinates shown in Fig. 3. Both methane and oxygen decompose gradually, as shown in Fig 5. The formation and consumption of CO can be easily observed owing to the higher thermal and spatial dispersion/resolution of the weak flame.

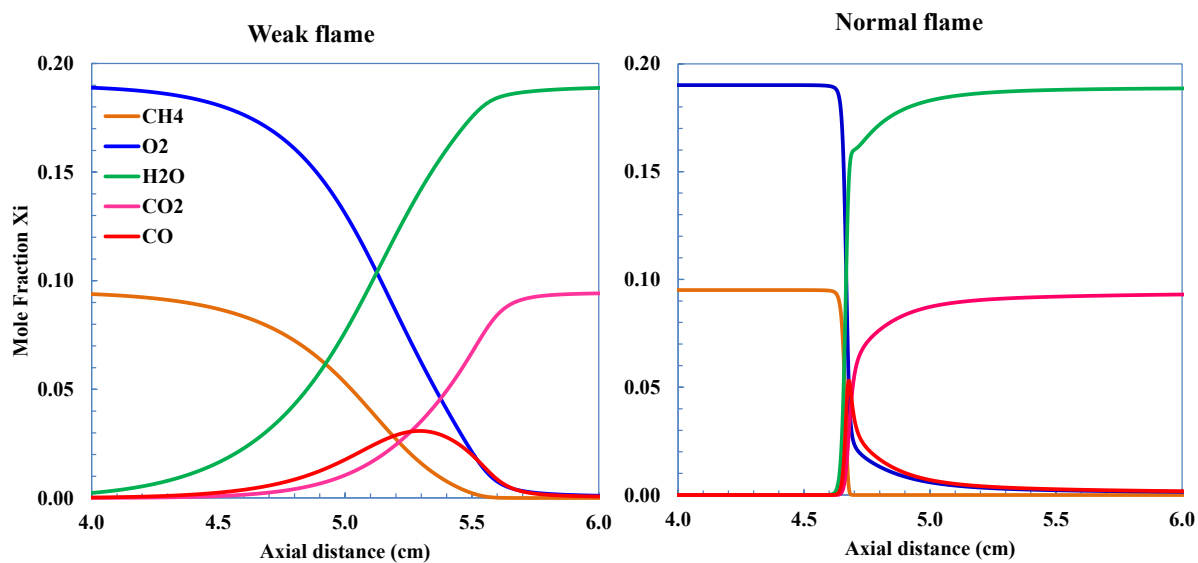


Figure 5 Major species profile for stoichiometric methane-air weak and normal flames

Fig. 6 shows the variation in the minor species for weak (unconventionally wide) and normal (conventionally thin) flames. The formation and consumption of CH<sub>2</sub>O could be easily observed because of the higher thermal and spatial dispersion/resolution of the weak flame. At the end of CH<sub>2</sub>O decomposition, the formation of OH and CH begins.

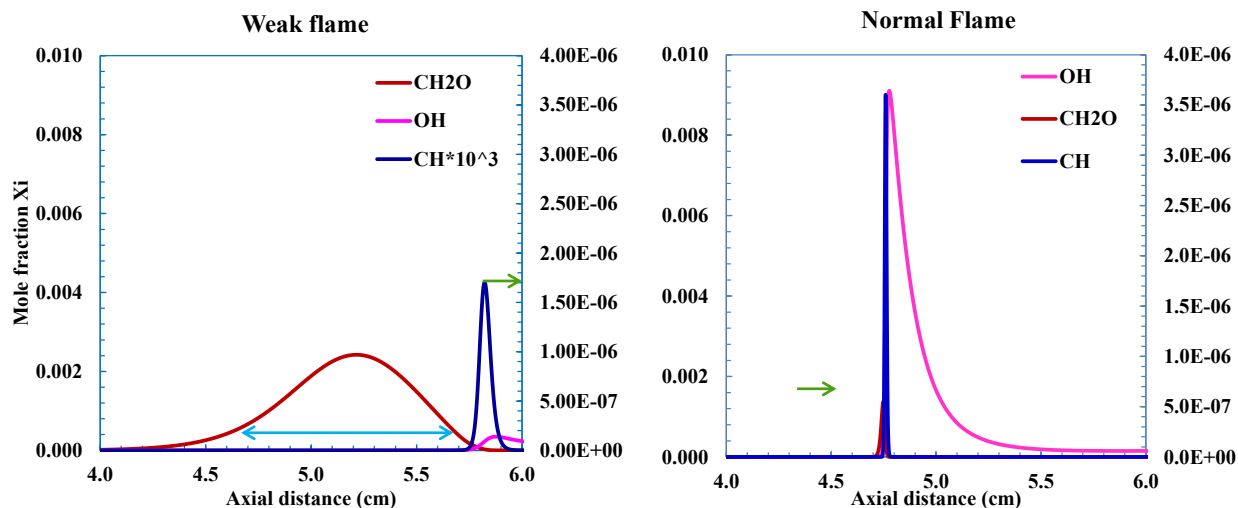


Figure 6 Minor species profile for stoichiometric methane-air weak and normal flames

## Mechanism testing with weak and normal flames

### Formaldehyde distribution

The formation and consumption of formaldehyde in weak and normal flames obtained from various detailed mechanisms are shown in Fig. 7. All the mechanisms revealed a wide CH<sub>2</sub>O zone for a weak flame and a narrow zone for a normal flame. The GRI mech 3.0 and the San Diego mech both exhibited a lower temperature decomposition of methane to form CH<sub>2</sub>O compared to USC mech II for weak flames. However, all these mechanisms provide the maximum mole fraction of CH<sub>2</sub>O at different temperatures. Significant scatter in the magnitude of the CH<sub>2</sub>O mole fraction as can be seen in Fig. 7. This is due to the low- and intermediate-temperature oxidation reaction subsets. For normal flames, the CH<sub>2</sub>O formation, consumption, and mole fractions obtained from these mechanisms were in good agreement. This is because of the emphasis on high-temperature oxidation. Normal flames contain a lower amount of CH<sub>2</sub>O than weak flames because of the formation of other species in other branches.

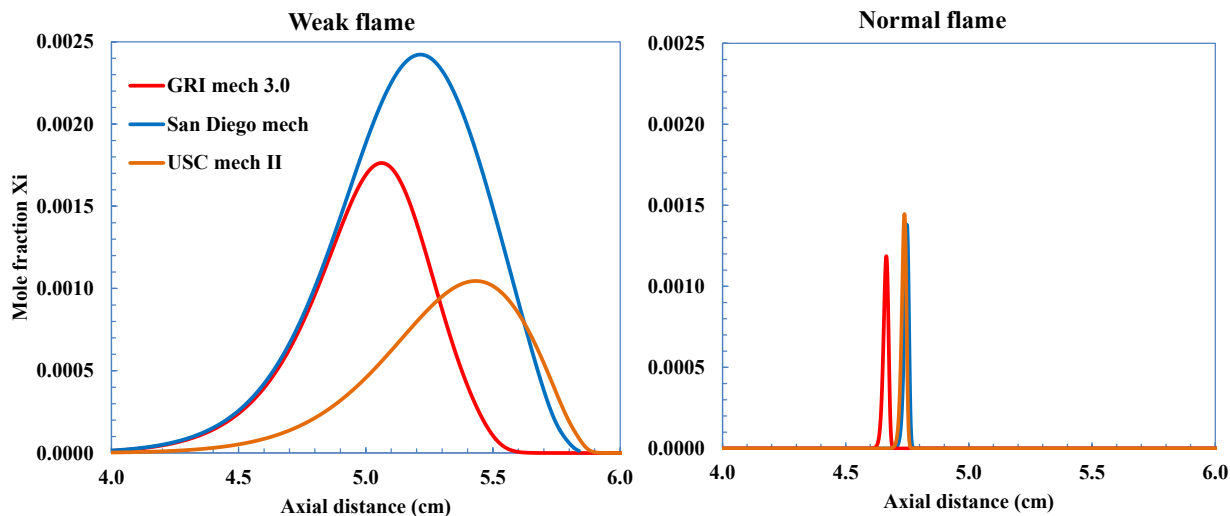


Figure 7 CH<sub>2</sub>O profile for stoichiometric methane-air weak and normal flames with various detailed mechanisms

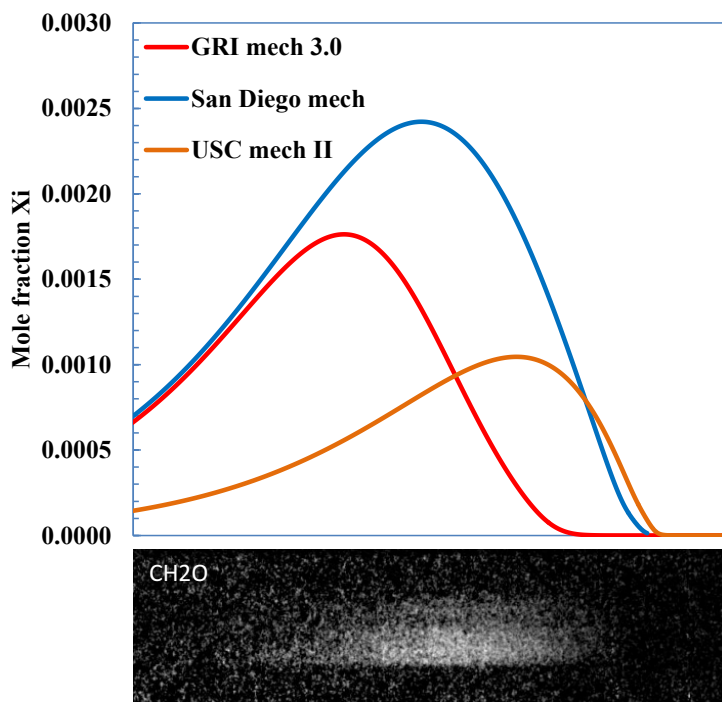


Figure 8 Comparison of LIF imaging of CH<sub>2</sub>O for stoichiometric methane-air weak flame (top) and computations with various detailed mechanisms (bottom). Experimental data are taken from Shimizu et al. [16].

Figure 8 shows the comparison of the LIF imaging of CH<sub>2</sub>O for stoichiometric methane-air weak flames and computations with various mechanisms. The figure shows a qualitative agreement between the experimental values and the San Diego mech. However, other mechanisms have predicted the widespread use of formaldehyde in weak flames.

## Hydroxyl distribution

Compared to the normal flame, the hydroxyl (OH) formation begins after a significant decay in the CH<sub>2</sub>O mole fraction in the weak flame (see Fig. 9). Such an insight is extremely difficult to capture from conventional normal flames. Although the OH formation began at two different physical locations in these flames, it began at the same gas temperature of 1200 K. In normal flame cases, the flame temperature reached ~1200 K once CH<sub>2</sub>O began to decay. However, for a weak flame, the wall temperature also contributed to the initiation of OH formation.

The OH initiation temperature was almost the same for the San Diego mech and the USC mech II. However, the GRI mech 3.0, revealed an early initiation of thermal coordinates (approximately 25 K).

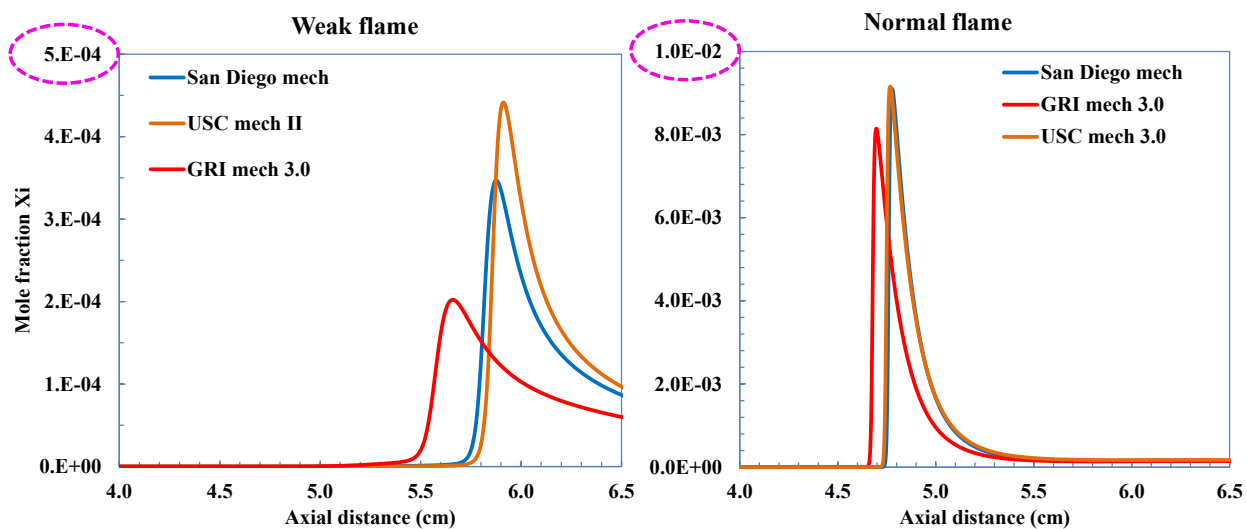


Figure 9 OH profile for stoichiometric methane-air weak and normal flames with various detailed mechanisms

Figure 10 shows the comparison of the LIF imaging of OH for stoichiometric methane-air weak flame and computations with various mechanisms. The figure shows a qualitative agreement between the experimental values and the San Diego mech and USC mech II. However, the GRI mech 3.0 predicts the earlier initiation of OH in weak flames.

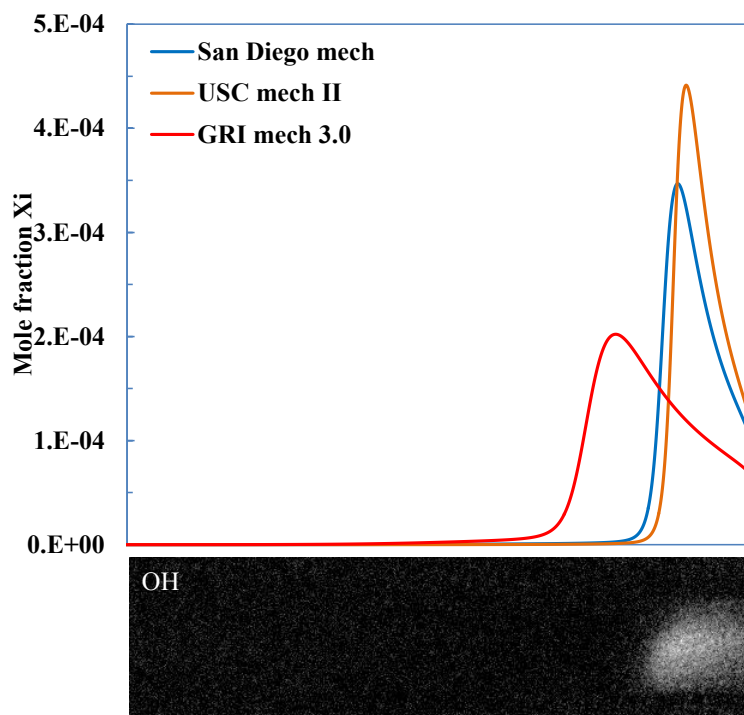


Figure 10 Comparison of LIF imaging of OH in methane-air weak flame (top) and computations with various detailed mechanisms (bottom). Experimental data are taken from Shimizu et al. (2017) [16].

### CH distribution

The CH formation began simultaneously with the OH (see Fig. 9) formation in both flames, at a gas temperature of 1200 K. In the normal flame, the flame temperature reached ~1200 K once CH<sub>2</sub>O began to decay. In contrast, in the case of a weak flame, the wall temperature also contributed to the initiation of CH formation.

The CH initiation temperature was almost the same in the San Diego mech and USC mech II, as shown in Fig. 11. However, GRI mech 3.0 reveals an early initiation of the thermal coordinates (approximately 25 K) in both flames.

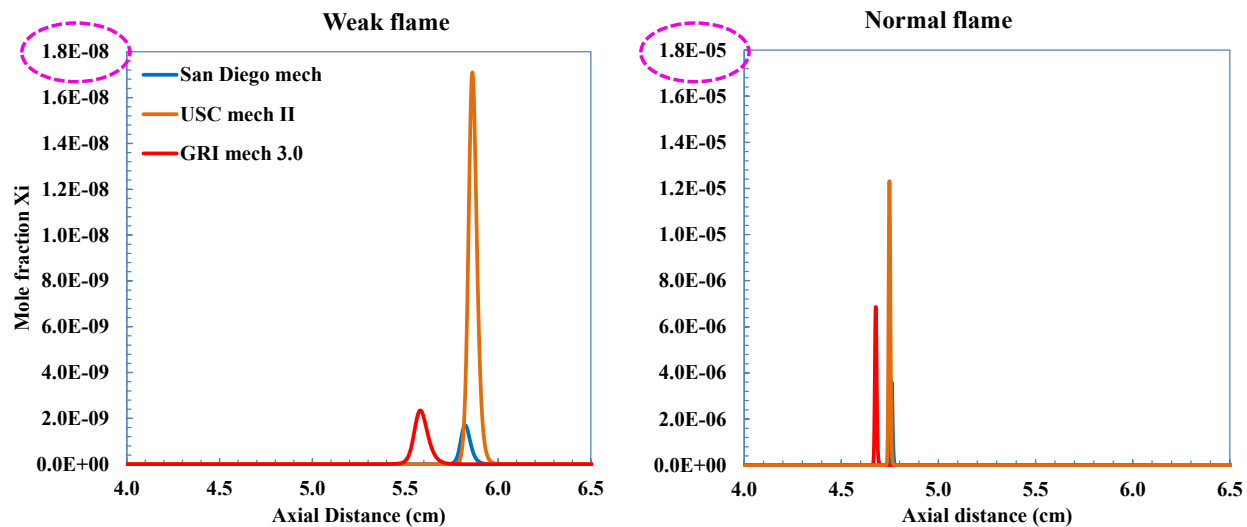


Figure 11 CH profile for stoichiometric methane-air weak and normal flames

Figure 12 shows the comparison of the direct photograph imaging of CH for stoichiometric methane-air weak flame and computations with various mechanisms. The figure shows a qualitative agreement between the experimental values and the San Diego mech. However, other mechanisms also predicted the CH formation accurately in weak flames.

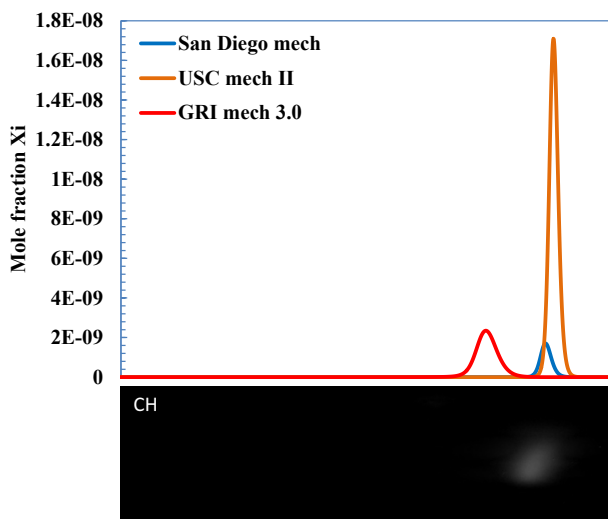


Figure 12 Comparison of direct imaging of CH in methane-air weak flame (top) and computations with various detailed mechanisms (bottom). Experimental data are taken from Shimizu et al. (2017) [16].

## Heat release rates

The heat release rates of the weak and normal flames were quantitatively distinct, as shown in Fig. 13. Various heavy-hydrocarbon fuels undergo two- to three-stage combustions. Methane, being the simplest hydrocarbon is popular to have only stage combustion. However, the heat release rate distribution with two peaks suggests that GRI mechanism 3.0 shows a clear two-stage combustion for the methane-air mixture. On the contrary, the other mechanisms exhibited a wide distribution of low-magnitude heat with two peak magnitudes. This necessitates a sincere review of the low- and intermediate-temperature chemistries of these mechanisms.

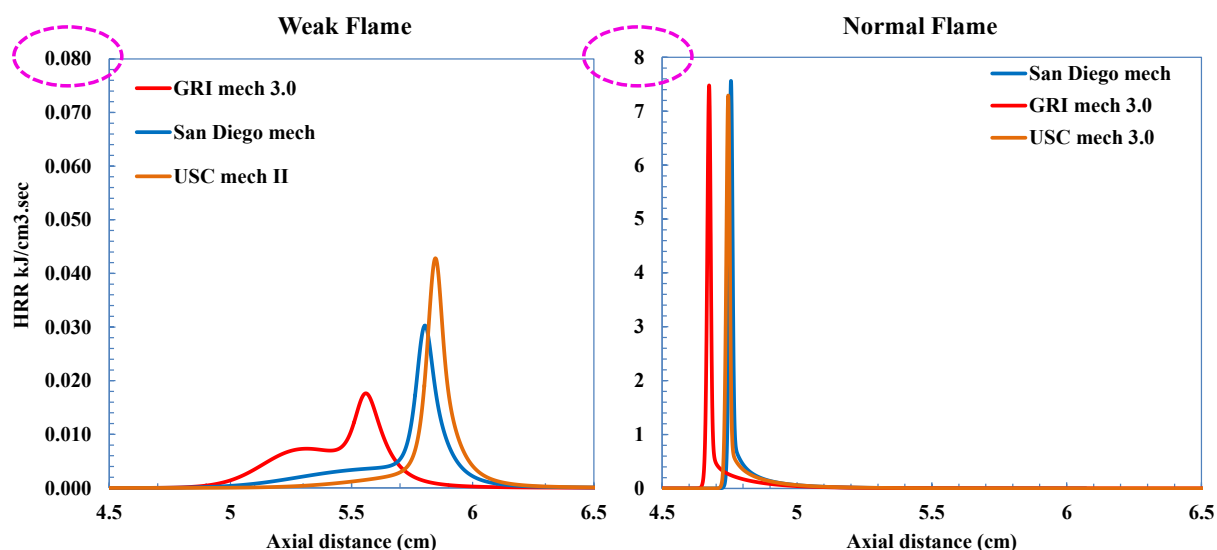


Figure 13 Heat release rate profiles for stoichiometric methane-air weak and normal flames with various detailed mechanisms

## Conclusions

Testing various detailed mechanisms of the microflow combustor helps in revealing physical insights into the reaction zone distribution. For stoichiometric methane-air mixture, weak and normal flames can be stabilized to study intermediate- and high-temperature oxidations. All the mechanisms produced similar results. The San Diego mech and the USC mech II were found to be in close qualitative agreement with the experiments. Only the GRI mech 3.0 exhibited two-stage combustion of methane and air flames. Additionally, an early initiation of OH and CH was exhibited compared to the other two mechanisms and experiments. Therefore, further sincere investigations of the low- and intermediate-temperature chemistries are required.

## Acknowledgment

This work was supported by the Deanship of Scientific Research (DSR), King Abdulaziz University, Jeddah, under Grant No. (D-079-135-1440). We gratefully acknowledge the technical and financial support provided by the DSR.

## References

- Curran, H. J., Fischer, S. L., and Dryer, F. L.** 2000. The reaction kinetics of dimethyl ether. II: Low-temperature oxidation in flow reactors. *International Journal of Chemical Kinetics*. 32(12): 741-59.
- Fischer, S. L., Dryer, F. L., and Curran, H. J.** 2000. The reaction kinetics of dimethyl ether. I: High-temperature pyrolysis and oxidation in flow reactors. *International Journal of Chemical Kinetics*. 32(12): 713-40.
- Johnson, M. V., Goldsborough, S. S., Serinyel, Z., O'Toole, P., Larkin, E., O'Malley, G., and Curran, H. J.** 2009. A Shock Tube Study of n- and iso-Propanol Ignition. *Energy & Fuels*. 23(12): 5886-98.
- Metcalf, W. K., Burke, S. M., Ahmed, S. S., and Curran, H. J.** 2013. A Hierarchical and Comparative Kinetic Modeling Study of C1 – C2 Hydrocarbon and Oxygenated Fuels. *International Journal of Chemical Kinetics*. 45(10): 638-75.
- Westbrook, C. K., Pitz, W. J., Curran, H. C., Boercker, J., and Kunrath, E.** 2001. Chemical kinetic modeling study of shock tube ignition of heptane isomers. *International Journal of Chemical Kinetics*. 33(12): 868-77.
- Zhao, Z., Chaos, M., Kazakov, A., and Dryer, F. L.** 2008. Thermal decomposition reaction and a comprehensive kinetic model of dimethyl ether. *International Journal of Chemical Kinetics*. 40: 1-18.
- Al-Dawody, M. F., Al-Farhany, K. A., Hamza, N. H., and Hamzah, D. A.** 2021. Numerical study for the spray characteristics of diesel engine powered by biodiesel fuels under different injection pressures. *Journal of Engineering Research*. 10(1B): 264-89.
- Fayad, M. A.** 2021. Investigation of the impact of injection timing and pressure on emissions characteristics and smoke/soot emissions in diesel engine fuelling with soybean fuel. *Journal of Engineering Research*. 9(2).
- Yu, H., Wang, W., Duan, S., and Sun, P.** 2021. Quantitative analysis of combustion process of marine dual fuel engine under the framework of iconology. *Journal of Engineering Research*. 9(4B).
- Chen, J. Y.** 1988. A General Procedure for Constructing Reduced Reaction Mechanisms with Given Independent Relations. *Combustion Science and Technology*. 57(1-3): 89-94.
- Lu, T. and Law, C. K.** 2005. A directed relation graph method for mechanism reduction. *Proceedings of the Combustion Institute*. 30(1): 1333-41.
- Kamada, T., Nakamura, H., Tezuka, T., Hasegawa, S., and Maruta, K.** 2014. Study on combustion and ignition characteristics of natural gas components in a micro flow reactor with a controlled temperature profile. *Combustion and Flame*. 161(1): 37-48.
- Maruta, K., Kataoka, T., Kim, N. I., Minaev, S., and Fursenko, R.** 2005. Characteristics of combustion in a narrow channel with a temperature gradient. *Proceedings of the Combustion Institute*. 30(2): 2429-36.
- Nakamura, H., Yamamoto, A., Hori, M., Tezuka, T., Hasegawa, S., and Maruta, K.** 2013. Study on pressure dependences of ethanol oxidation by separated weak flames in a micro flow reactor with a controlled temperature profile. *Proceedings of the Combustion Institute*. 34(2): 3435-43.
- Oshibe, H., Nakamura, H., Tezuka, T., Hasegawa, S., and Maruta, K.** 2010. Stabilized three-stage oxidation of DME/air mixture in a micro flow reactor with a controlled temperature profile. *Combustion and Flame*. 157(8): 1572-80.

**Shimizu, T., Nakamura, H., Tezuka, T., Hasegawa, S., and Maruta, K.** 2017. OH and CH<sub>2</sub>O Laser-Induced Fluorescence Measurements for Hydrogen Flames and Methane, n-Butane, and Dimethyl Ether Weak Flames in a Micro Flow Reactor with a Controlled Temperature Profile. *Energy & Fuels*. 31(3): 2298-307.

**Tsuboi, Y., Yokomori, T., and Maruta, K.** 2009. Lower limit of weak flame in a heated channel. *Proceedings of the Combustion Institute*. 32(2): 3075-81.

**Yamamoto, A., Oshibe, H., Nakamura, H., Tezuka, T., Hasegawa, S., and Maruta, K.** 2011. Stabilized three-stage oxidation of gaseous n-heptane/air mixture in a micro flow reactor with a controlled temperature profile. *Proceedings of the Combustion Institute*. 33(2): 3259-66.

**Kee, R., Grear, J., Smooke, M., Miller, J., and Meeks, E.** 1985. PREMIX : A FORTRAN Program for Modeling Steady Laminar One-Dimensional. SANDIA National Laboratories ..., (April): 1-87.

**Kee, R. J., Grear, J. F., Smooke, M. D., and Miller, J. A.**, A FORTRAN Program for Modeling Steady Laminar One-Dimensional Premixed Flames. 1993.

**Mechanism, S. D.**, Chemical-kinetic mechanisms for combustion applications. 2011.

Wang, H., You, X., Joshi, A. V., Davis, S. G., Laskin, A., Egolfopoulos, F., and Law, C. K., High-Temperature Combustion Reaction Model of H<sub>2</sub>/CO/C<sub>1</sub>-C<sub>4</sub> Compounds. 2007.

Smith, G. P., Golden, D. M., Frenklach, M., N. W. Moriarty, B. E., Goldenberg, M., Bowman, C. T., Hanson, R. K., Song, S., Jr, W. C. G., Lissianski, V. V., and Qin, Z., GRI mech 3.0. 2000.

**Onda, T., Nakamura, H., Tezuka, T., Hasegawa, S., and Maruta, K.** 2019. Initial-stage reaction of methane examined by optical measurements of weak flames in a micro flow reactor with a controlled temperature profile. *Combustion and Flame*. 206: 292-307.